Geogr. Fis. Dinam. Quat.
45 (2022). 185-195, suppl. mat. 1-4, 6 figg.

DOI 10.4461/ GFDQ.2022.45.7

LYUBA NOVI [1*], MARIA CRISTINA SALVATORE [1,2], FRANCESCO RAFFA [1],
FRANCESCA BIASCI [2], ANTONELLO PROVENZALE [1] & CARLO BARONI [1,2]

ZONATION OF WAVE-INDUCED EROSION THREAT OF A SANDY SHORELINE IN CENTRAL TUSCANY (ITALY) SUPPLEMENTARY MATERIAL

Relative importance of waves and tides forcing on cumulative sediment transport.

Numerical simulations of sediment transport due to the separate forcing of waves-only and tides-only are additionally carried out, to assess the relative importance of the two drivers on cumulative transport. The Delft3D-FLOW model (Deltares-Delft3D-FLOW, 2020) is applied on a depth-averaged 136*X*32 grid over coastal waters at the study site (fig. S1). For the waves-only case the model is coupled with the Delft3D-WAVE module, from which information is passed to FLOW to compute the wave-induced hydrodynamics effects and the related sand transport. In the wave-only case, all the hydrodynamic and wind forcing other than the wave-induced ones are suppressed by imposing constantly zero wind and zero boundary conditions on water levels, which translates in null flow. We further verified that no flow develops in this case by running a baseline simulation with the null-boundary conditions. Boundary conditions for waves (H_s = 0.9 m, θ_m = 213°, $T\,p$ = 6 s) and flow are both applied at the open boundary of the domain. For the tides-only case, only tidal boundary conditions force the hydrodynamics at the open boundary in the FLOW module. Amplitude and phase of the K1 and M2 constituents (the main ones) are obtained as yearly values by analyzed hourly measurements from the National Tidal Gauge Network - ISPRA, for the Livorno station (tidal analysis data available at https://www.mareografico.it/en/data-archive.html. Typical tidal conditions are computed as the average phase and amplitudes over 2001-2014 and imposed at the model boundary. M2 amplitude and phase are 9.07 cm and 190°, with standard deviation 0.76 cm and 27.8°; K1 amplitude and phase are 3.55 cm and 168.6°, with standard deviation 0.13 cm and 4.2°. In both the wave-only and the tides-only simulations, the sediment (sand) median diameter is set at 0.2 mm, the dry bed density is set at 1600 kg/m^3, the specific density is set at 2650 kg/m^3. The bottom stress enhancement due to waves is computed using the formulation of (Fredsøe, 1984) available in the Delft3D-FLOW module. Through numerical simulations, we compared the yearly cumulative and instantaneous total sediment transport (bed load+suspended), due to tides only and to waves only. The non-dimensional ratio of the cumulative total transport for tides-only onto the one due to waves-only ranges from (order of magnitudes) 10^{-8} and 10^{-14} per year (fig. S2) at all the 11 observation points distributed on the northern part of the domain (closer to the tide station) within the closure depth. Values for the corresponding ratios of instantaneous total transport is also very small, ranging from 10^{-7} and 10^{-13} (fig. S3). The assumption of negligible tides when compared to the wave forcing on sediments is numerically verified and in line with previous knowledge on the small tidal

[1] *CNR-IGG, Istituto di Geoscienze e Georisorse, Via G. Moruzzi 1, 56124, Pisa, Italy.*

[2] *Dipartimento di Scienze della Terra, University of Pisa, Via Santa Maria, 53, 56126 Pisa, Italy.*

* *Corresponding author: L. Novi (ljuba.novi.res@gmail.com)*

This study was funded by the National Research Council of Italy and the EU H2020 project ECOPOTENTIAL grant number 641762. Part of this study has been conducted using the E.U. Copernicus Marine Service Information. The work has been performed in the framework of the 32° Cycle of the PhD Course in Earth Sciences at the University of Pisa, Italy.

Authors contributions: LN conceived the study, performed the calculations, and wrote the manuscript. MCS detected the shoreline positions over 1988-2013. MCS and CB evaluated the advance and retreat of the shoreline at different time intervals. AP, FR, MCS, and CB reviewed the manuscript. FB contributed detecting some of the shoreline positions. AP provided funding.

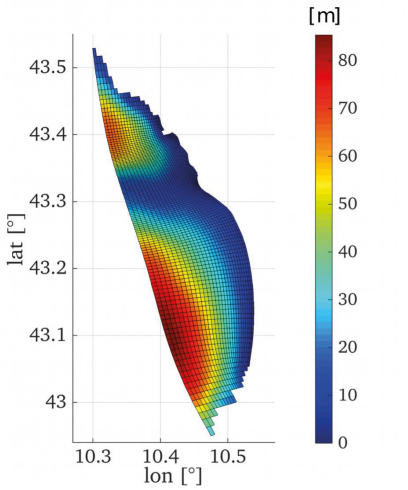

FIG. S1 - Numerical grid used for the sediment transport simulations. The boundary conditions are applied at the open boundary boundary (western boundary). The water depth (positive downwards) at the latest time step is also shown for reference.

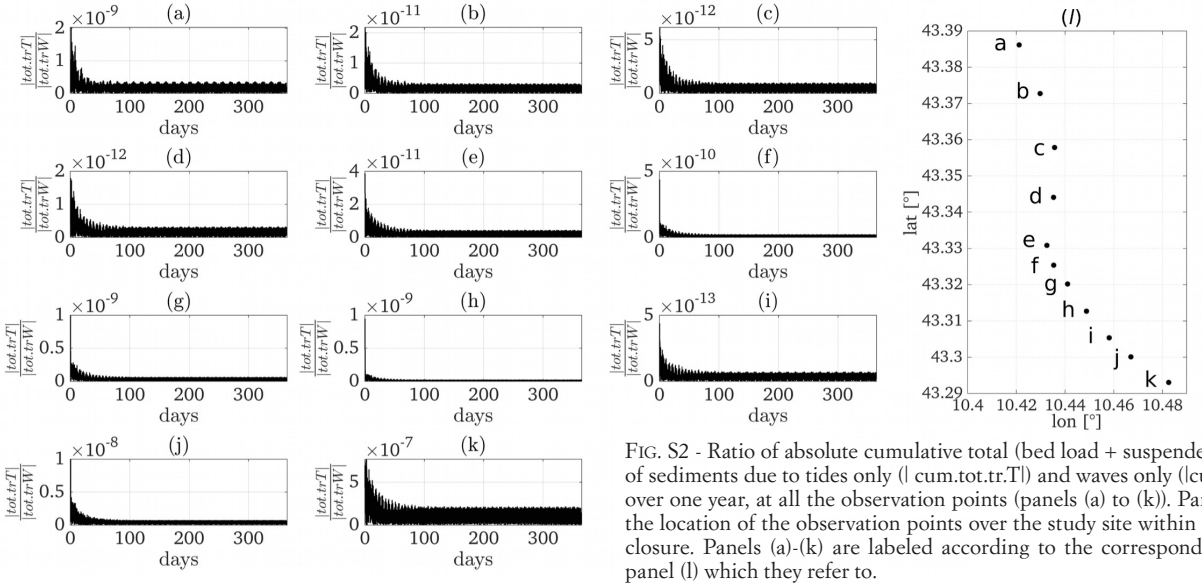

FIG. S2 - Ratio of absolute cumulative total (bed load + suspended) transport of sediments due to tides only (| cum.tot.tr.T|) and waves only (|cum.tot.tr.W|) over one year, at all the observation points (panels (a) to (k)). Panel (l) shows the location of the observation points over the study site within the depth of closure. Panels (a)-(k) are labeled according to the corresponding point in panel (l) which they refer to.

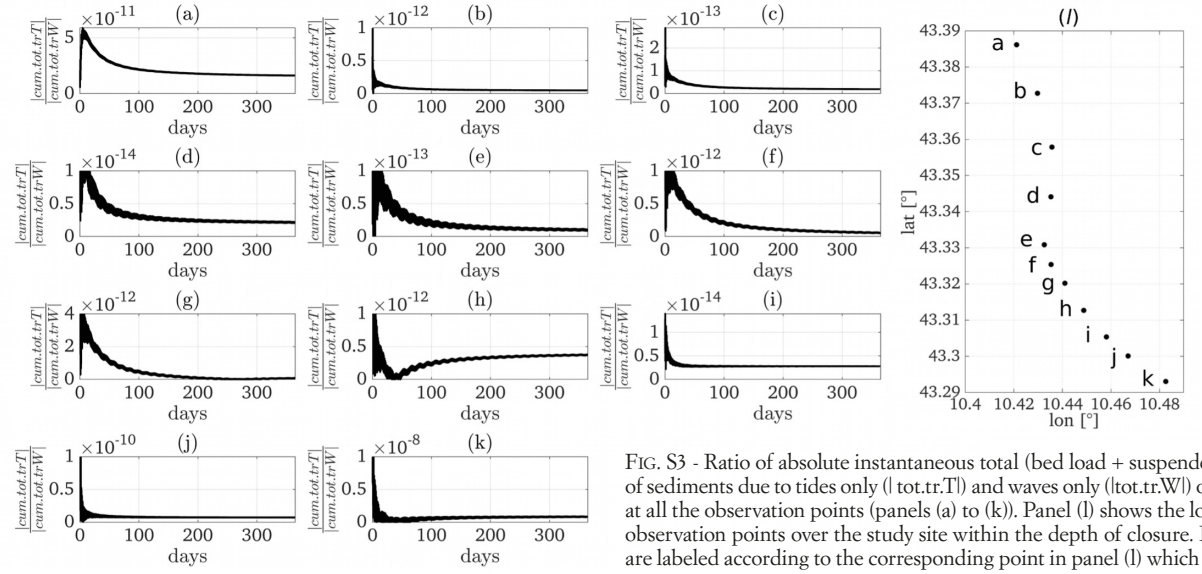

FIG. S3 - Ratio of absolute instantaneous total (bed load + suspended) transport of sediments due to tides only (| tot.tr.T|) and waves only (|tot.tr.W|) over one year, at all the observation points (panels (a) to (k)). Panel (l) shows the location of the observation points over the study site within the depth of closure. Panels (a)-(k) are labeled according to the corresponding point in panel (l) which they refer to.

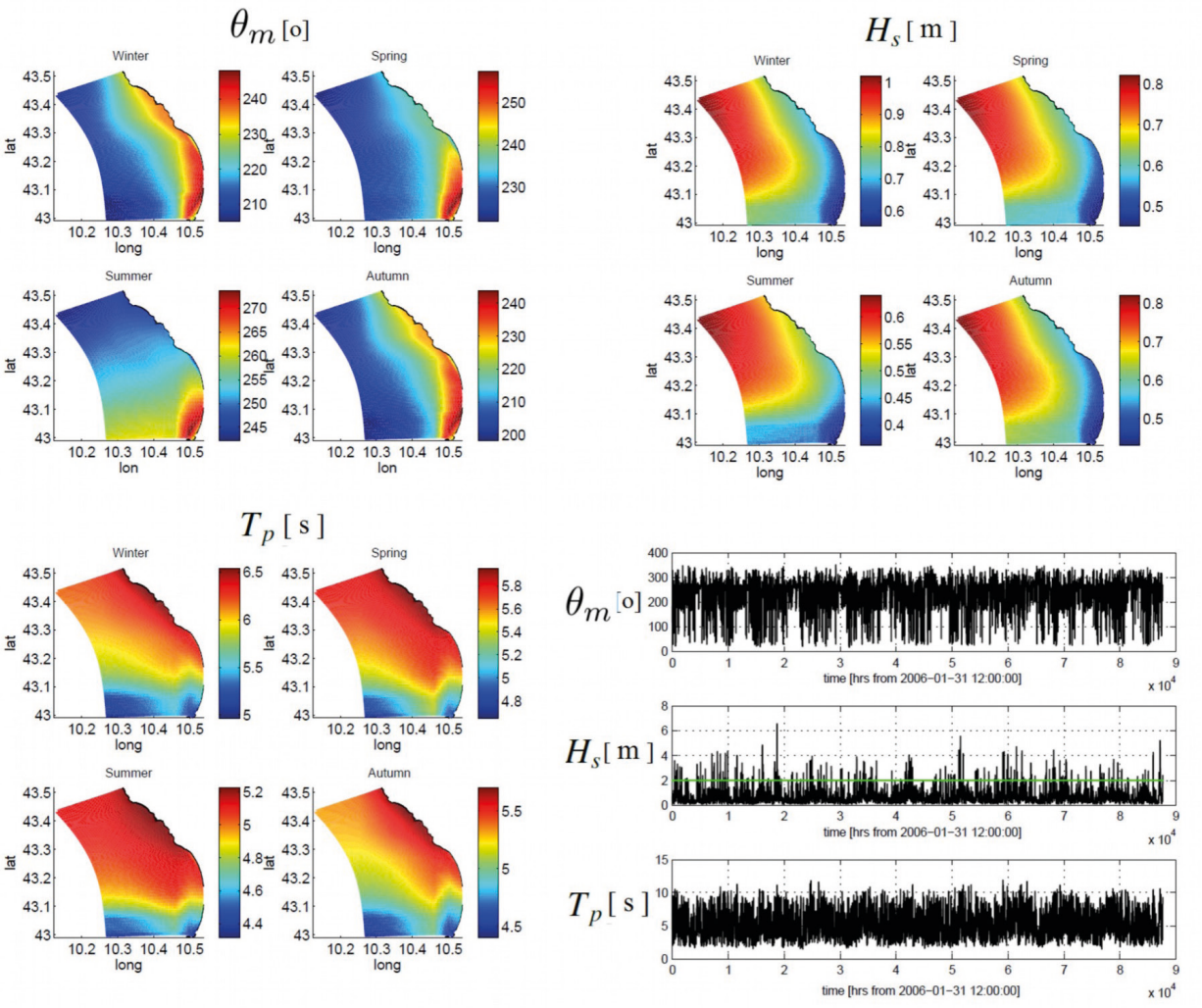

FIG. S4 - wave mean seasonal climatology computed over 2006-2016 for the 1/24° data after a linear remapping on the overall computational grid.

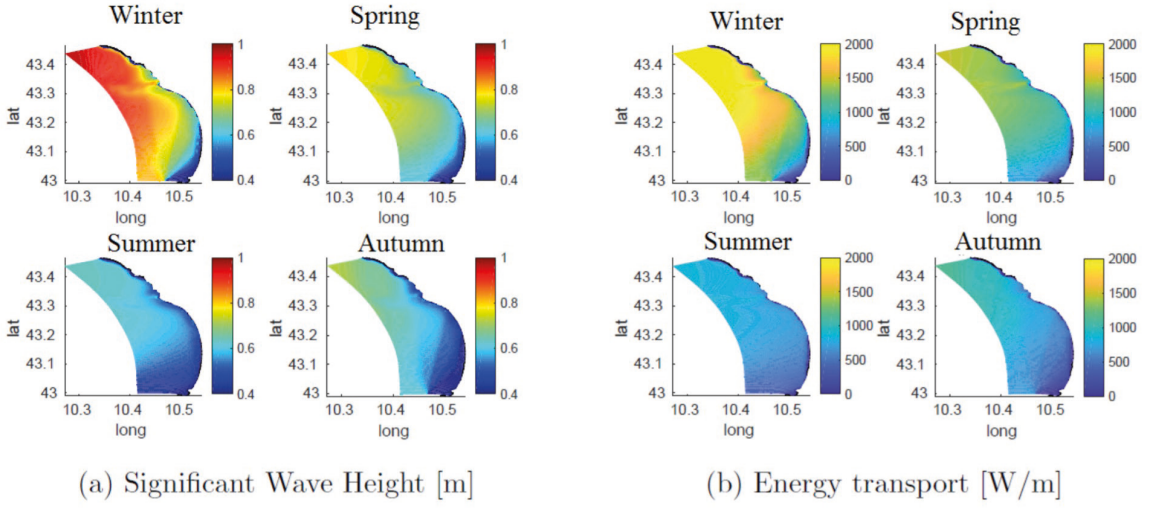

FIG. S5 - Simulations output for the nested domain, when seasonal climatology at high resolution over the decade 2006-2016 used as boundary conditions.

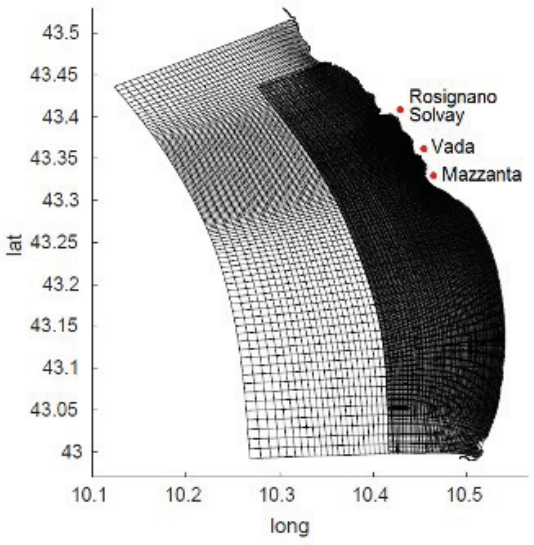

FIG. S6 - Computational grids: the mid-resolution grid (lighter area) covers the physiographic unit. The nested high-resolution grid (darker area) reaches a resolution of 29 m in the coastal zone. The geographical coordinates (long-lat) are expressed in decimal degrees. The red spots indicate the location of the places written next to them for reference.

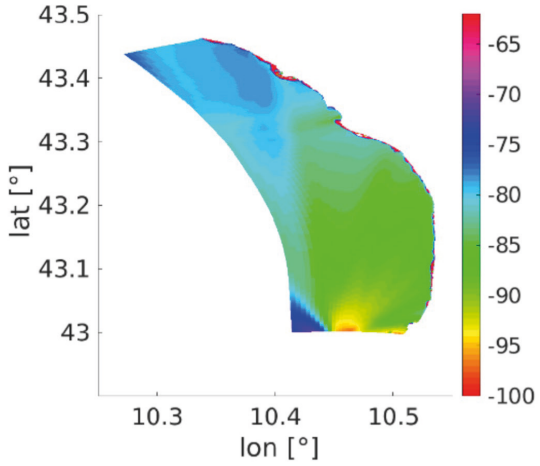

FIG. S7 - Relative percentage error between the output obtained with the LR source and with the HR one, for the winter condition over 2006-2016. The colorbar represent % values.

amplitudes in the area.

2006-2016 wave seasonal climatology in Central Tuscany, Italy.

The wave mean seasonal climatology is computed over the decade 2006-2016 for the 1/24° data (fig. S4) after a linear remapping on the overall computational grid. A seasonal variability of the significant wave height is found over the entire area, with the highest off-shore significant wave height H_s above 1 m occurring in winter. Winter values of H_s remains above 0.8 m for latitudes higher 43.3°, i.e. north of Mazzanta and throughout Rosignano coastline. Lower values ofH_s are found south of 43.3° but still above 0.55 m in winter. The same spatial pattern of significant wave height persists for all the seasons but with a sensitive seasonal variation of absolute values. The lowest H_s occurs during summer, when the offshore values decrease of more than about 30% and the nearshore values never exceed 0.6 m. Longer periods are associated with winter higher wave heights. Mean wave directions are mainly from S-SW for the winter mean climatology, rotating SW-W during summer.

The 2006-2016 seasonal mean climatology numerical output of H_s and *Etr* for the nested model are reported in fig. S5. A clear variability is found in agreement with the overall behavior obtained from the 1/24° data, and a refined spatial representation. The highest values of significant wave height and the strongest average energy transport are found in winter. The winter *Etr* between Vada and Mazzanta reaches more than twice the *Etr* summer values in the same locations, i.e. about 2000 [w/m] in winter and about 850 [W/m] in summer when it is at its seasonal minimum. Intermediate values are found for spring (more energetic) and autumn (less energetic). The spatial variability persists all year round. The choice of the isobath on which L and C are computed, is constrained by the closure depth (deeper limit) and the wave breaking depth (shallower limit), but in practice the quality of the bathymetric data puts a limit to the knowledge of the shallower isolines. However, the values chosen here are arbitrary within these limits and other values could alternatively have been used in the same range. Results in main text are shown for i = 6.36 m.

REFERENCES

DELTARES-DELFT3D-FLOW (2020) - *User Manual: Simulation of multi-dimensional hydrodynamic flows and transport phenomena, including sediments*. Available at: https://content.oss.deltares.nl/delft3d/manuals/ Delft3D-FLOW_User_Manual.pdf.

DELTARES-DELFT3D-WAVE (2020) - *User Manual: Simulation of short-crested waves with SWAN*. Available at: https://content.oss.deltares.nl/ delft3d/manuals/Delft3D-WAVE_User_Manual.pdf.

FREDSØE J. (1984) - *Turbulent boundary layer in wave-current interaction*. Journal of Hydraulic Engineering, 110, 1103-1120.